

See discussions, stats, and author profiles for this publication at: <https://www.researchgate.net/publication/283420477>

Application of Support Vector Machines for Landuse Classification Using High-Resolution RapidEye Images: A Sensitivity Analysis

Article in *European Journal of Remote Sensing* · November 2015

DOI: 10.5721/EuJRS20154823

CITATIONS

22

READS

469

3 authors:



Mustafa Üstüner

35 PUBLICATIONS 58 CITATIONS

[SEE PROFILE](#)



Fusun Balik Sanli

Yildiz Technical University

65 PUBLICATIONS 220 CITATIONS

[SEE PROFILE](#)



Barnali Dixon

University of South Florida St. Petersburg

40 PUBLICATIONS 879 CITATIONS

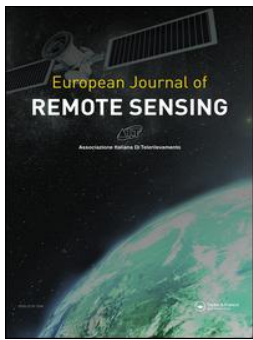
[SEE PROFILE](#)

Some of the authors of this publication are also working on these related projects:



Project

Determination and Monitoring of Spatial and Temporal Changes of Soil moisture and Roughness Using Microwave Satellite Images (RADARSAT-2) [View project](#)



Application of Support Vector Machines for Landuse Classification Using High-Resolution RapidEye Images: A Sensitivity Analysis

Mustafa Ustuner, Fusun Balik Sanli & Barnali Dixon

To cite this article: Mustafa Ustuner, Fusun Balik Sanli & Barnali Dixon (2015) Application of Support Vector Machines for Landuse Classification Using High-Resolution RapidEye Images: A Sensitivity Analysis, European Journal of Remote Sensing, 48:1, 403-422, DOI: [10.5721/EuJRS20154823](https://doi.org/10.5721/EuJRS20154823)

To link to this article: <http://dx.doi.org/10.5721/EuJRS20154823>



© 2015 The Author(s). Published by Taylor & Francis.



Published online: 17 Feb 2017.



[Submit your article to this journal](#)



Article views: 154



[View related articles](#)



[View Crossmark data](#)



Citing articles: 1 [View citing articles](#)



Application of Support Vector Machines for Landuse Classification Using High-Resolution RapidEye Images: A Sensitivity Analysis

Mustafa Ustuner^{1*}, Fusun Balik Sanli¹ and Barnali Dixon²

¹Department of Geomatic Engineering, Yildiz Technical University, 34220 Esenler, Istanbul, Turkey

²Department of Environmental Science, Policy and Geography, University of South Florida,
St. Petersburg, Florida 33701, USA

*Corresponding author, e-mail address: mustuner@yildiz.edu.tr

Abstract

The classification accuracy of remotely sensed data and its sensitivity to classification algorithms have a critical importance for the geospatial community, as classified images provide the base layers for many applications and models. Support Vector Machines (SVMs), a non-parametric statistical learning method that has recently been used in numerous applications in image processing. The SVMs need user-defined parameters and each parameter has different impact on kernels hence the classification accuracy of SVMs is based upon the choice of the parameters and kernels. The objective of this study is to investigate the sensitivity of SVM architecture including internal parameters and kernel types on landuse classification accuracy of RapidEye imagery for the study area in Turkey. Four types of kernels (linear, polynomial, radial basis function, and sigmoid) were used for the SVM classification. A total of 63 different models were developed and implemented for sensitivity analysis of SVM architecture. The traditional Maximum Likelihood Classification (MLC) method was also performed for comparison. The classification accuracies of the best model for each kernel type and MLC are 85.63%, 83.94%, 83.94%, 83.82% and 81.64% for polynomial, linear, radial basis function, sigmoid kernels and MLC, respectively. The results suggest that the choice of model parameters and kernel types play an important role on SVMs classification accuracy. Best model of polynomial kernel outperformed all SVMs models and gave the highest classification accuracy of 85.63% with RapidEye imagery.

Keywords: Support Vector Machines, RapidEye, landuse classification, sensitivity, kernel.

Introduction

Turkey's economy is greatly dependent upon agricultural productivity. Based upon the 2006 CORINE (Coordination of Information on the Environment) landuse/landcover (LULC) data, Turkey consists of 42% agricultural and 54% forestry and semi-natural vegetation areas [EEA, 2010]. For sustainable agriculture and food production as well as

the development of effective policies, accurate and reliable information regarding crop yields and soil conditions of agricultural fields are essential.

In Turkey, agricultural statistical data such as yield and acreage which is based on the declarations of farmers is collected by the local technical staff of the Ministry of Food, Agriculture and Livestock. The Government subsidies are provided to the farmers based on their declarations of crop types, yield and acreage [Ünal et al., 2006]. These data sometimes could be considered as unreliable due to false declarations from farmers. Therefore, decision makers and local authorities need the accurate and reliable information regarding the LULC for strategic planning and sustainable management of natural resources.

Remote sensing technology offers a viable solution in providing accurate, reliable and up-to-date information about crop monitoring and yield, using new generations of high-resolution remote sensing data and image classification algorithms [McNairn et al., 2002; Rogan and Chen, 2004; Soria-Ruiz et al., 2009]. Five meter spatial resolution data is required for land use/cover problems at high-ordered thematic levels [Rogan and Chen, 2004]. Three meter or lower spatial resolution satellite images such as RapidEye or SPOT (French: Satellite Pour l'Observation de la Terre) are often used for precision farming [ARECA, 2010]. The RapidEye system is helpful to monitor agricultural landuse at the regional and/or global scale due to its spatial resolution and red-edge channel which offers improved separability of crop types. One of the main missions of the RapidEye program was to provide up-to-date and reliable information for precision farming technology [Tyc et al., 2005]. RapidEye's red-edge and near-infrared bands were particularly designed for monitoring and identification of crop types in agricultural areas [Weeber, 2010]. RapidEye images have been successfully used for crop classification in some recent studies by Conrad et al. [2014], Forkuor et al. [2014], Abdikan et al. [2015] and Löw et al. [2015]. However, before recommending the adoption of remote sensing based methodologies to aid the Ministry of Food, Agriculture and Livestock in Turkey with better decision support systems (DSS), or any other governmental organizations around the world, it is critical that the suitability of such an application is determined using extensive sensitivity analysis.

Image classification is the most common method used to derive LULC information routinely and cost effectively [Huang et al., 2002; Mathur and Foody, 2008]. Numerous image classification algorithms exist. Over the past three decades, many studies have been conducted to analyze classification accuracies of various image processing algorithms [Townshend, 1992; Hall et al., 1995; Huang et al., 2002] and consequently new and improved image classification algorithms have become available. Maximum Likelihood Classifier (MLC), Decision Trees (DT) and Artificial Neural Network (ANN) classifiers are considered as popular classifiers over the last few decades [Huang et al., 2002]. Relatively newer classification algorithms include Random Forest (RT), Support Vector Machines (SVMs), Relevance Vector Machines (RVM) and Incremental import vector machines (I'VM) [Pal, 2012; Roscher et al., 2012; Tigges et al., 2013; Löw et al., 2013; Adelabu et al., 2014]. Conventional parametric method like MLC is based on statistical theory and assumes a multivariate normal distribution for each class [Mather, 2001; Huang et al., 2002; Otukey and Blaschke, 2010]. In case of data that has non-normal distribution (which is common with LULC data), the parametric classifiers may fail since the inability to resolve interclass confusion. This inability is the major limitation of parametric classifiers [Watanachaturaporn et al., 2008; Otukey and Blaschke, 2010; Pal, 2012]. Nonparametric classifiers like SVMs

which do not rely on any assumptions for the class distributions of data, could overcome the aforementioned limitations of parametric classifiers [Kavzoglu and Colkesen, 2009; Mountrakis et al., 2011; Pal, 2012]. SVMs, based on statistical learning theory, have been successfully applied to classify images [Huang et al., 2002; Pal and Mather, 2004; Dixon and Candade, 2007; Kavzoglu and Colkesen, 2009].

In recent years, the SVMs have been actively utilized for the classification of remotely sensed data for many purposes [Schuster et al., 2012; Adam et al., 2014; Adelabu et al., 2014; Abdikan et al., 2015; Schuster et al., 2015]. Schuster et al. [2012] tested the potential use of RapidEye rededge channel for improving LU classification. Adam et al. [2014] investigated the potential use of SVM and RF on LULC classification of RapidEye imagery. Adelabu et al. [2014] assessed the impact of the red edge channel of Rapideye imagery to discriminate different levels of insect defoliation in an African savanna by SVM and RF. Abdikan et al. [2015] examined the contribution of dual-polarized synthetic aperture radar (SAR) to optical data of RapidEye for the LU classification. Schuster et al. [2015] performed the SVMs classification of RapidEye and TerraSAR-X for classifying grassland habitats.

RapidEye's red-edge band, which is sensitive to chlorophyll content, provides the separability of landuse classes [Schuster et al., 2012; Tigges et al., 2013; Adelabu et al., 2014] and consequently increases the classification accuracy of vegetation, agriculture or forestry LULC classes. For example, Schuster et al. [2012] has examined the contribution of red-edge band on LU classification for the Berlin area and had 2.3% and 3.2% increases on overall accuracy of SVM and MLC classification, respectively, when the red-edge band is included. Tigges et al. [2013] has tested the multitemporal RapidEye satellite data for classification of urban trees and had 0.06, 0.10, 0.04 and 0.02 increases (0.05 in average) in overall kappa of four different SVM classifications when the red-edge band is included. Adelabu et al. [2014] has evaluated the impact of red-edge band from RapidEye image for classifying insect defoliation levels and obtained 19% and 21% increases on overall accuracy for SVM and RF classifications, respectively, when the red-edge band is included. These three studies found that presence of RapidEye's red-edge band increased the classification accuracy.

The primary objective of this research was assessing the applicability and sensitivity of SVM in classifying RapidEye images to enhance the agricultural landuse database for the Ministry of Food, Agriculture and Livestock in Turkey. The specific task of SVM sensitivity included analysis of internal parameters and kernel types on landuse classification accuracy.

Brief review of SVM applications

SVMs is a non-parametric statistical learning algorithm, which was originally aimed at binary classification by defining optimal hyperplane providing maximum margin separating two classes [Vapnik, 1995; Cortes and Vapnik, 1995; Huang et al., 2002]. In case of nonlinear classification, SVMs can perform the classification by using various types of kernels which turns nonlinear boundaries to linear ones in the high-dimensional space to define optimal hyperplane [Cortes and Vapnik, 1995; Huang et al., 2002; Pal and Mather, 2005; Mathur and Foody, 2008]. SVMs are based on the principle called Structural Risk Minimization (SRM) maximizing the margin between a separating hyperplane and data points closest to the hyperplane [Cortes and Vapnik, 1995; Vapnik, 1995; Huang et al., 2002]. Theoretically error penalty (C) that allows for misclassification plays an important role on SVM classification accuracy and researchers are currently focused on analyzing the

behaviour of this property more in depth [Petroopoulos et al., 2012]. The detailed information and mathematical representations of SVMs are provided in Vapnik [1995] and Cortes and Vapnik [1995].

Study area

Aydin Province, extending from 37°28' to 38°06' North latitudes and 27°01' to 28°56' East longitudes, is located in Turkey's Aegean region which has been famous for its fertile and productive farmlands since ancient times (Fig. 1). The central and western part of the province is covered with these farmlands.

The province, with its favourable climate and farmlands, enables every type of crop cultivation and has important agricultural potential for the country. Therefore, agriculture is an important source of income and approximately 55% of the whole population live off the agricultural activities. In the central part of the province, the annual crop pattern is mainly cotton, corn, vegetables and alfalfa in the summer and wheat is seen in the winter season.

The study area is comprised of approximately 107.38 km² of agricultural areas. It covers twelve landuse classes which are corn (first crop, second crop, third crop), cotton (well developed, moderate developed, weak developed), soil (wet, moist, dry), pasture and brush land mixed area, water surface and settlement area.

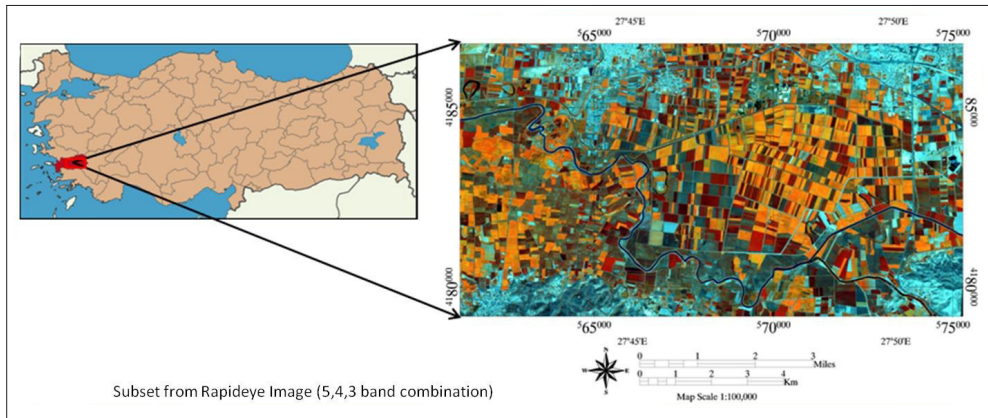


Figure 1 - Study area: Aydin Province, Turkey.

Materials and Methods

Data Sources

In this study, RapidEye imagery, which is a commercial optical Earth observation mission, was used. Since February 2009, RapidEye offers a data source having a large coverage with a 77 km swath width, frequent revisit intervals (5.5 days at nadir), high spatial resolution (6.5 m at nadir), and multispectral capabilities, in a single sun-synchronous orbit at an altitude of 630 km. RapidEye imagery is a constellation of five mini-satellites containing identical sensors in the same orbital plane. It provides five optical bands ranging between 400 nm to 850 nm. It is the first time that beside the standard channels of multi-spectral satellite sensors RapidEye imagery provides the red-edge band (690-730 nm) operationally

[Sandau, 2010; BlackBridge, 2013]. RapidEye delivers products at two different processing levels: RapidEye Basic (Level 1B) products are sensor level products with a minimal amount of processing (geometrically uncorrected) for customers who prefer to geo-correct the images themselves, and RapidEye Ortho products (Level 3A) are orthorectified products with radiometric, geometric and sensor corrections applied. The original spatial resolution of the RapidEye data are 6.5 m at nadir however RapidEye Ortho Product was delivered resampled to a 5 m spatial resolution [BlackBridge, 2013].

Input Data to SVMs

In this research, RapidEye Level 3A images acquired on the 23rd August, 2012 were used for parameter analysis of SVMs for LULC classification. The delivered scene was free of clouds and haze. The training dataset used in this study consisted of 11585 samples (pixels) (Tab.1). This is approximately 0.3% of the pixels in the entire study area.

Table 1 - Summary of the classes and pixels in the training dataset.

Class name	Training samples
First crop corn	1022
Second crop corn	1033
Third crop corn	445
Well-developed cotton	1121
Moderate developed cotton	1251
Weak developed cotton	1049
Wet soil	1300
Moist soil	1000
Dry soil	800
Water body	501
Settlement area	1450
Pasture and brush land mixed area	613
Total	11585

Ground Truth Data for Accuracy Assessment

In-situ data from 60 fields were collected using a handheld GPS at the acquisition date of satellite images to determine the mixing plant types. Once GPS points of the fields were used to identify the LULC classes (Tab. 2), ancillary data from Google earth was used to collect additional data for ground truthing (Figs. 2 and 3). The process of collection of additional ancillary data for ground truth was based on expert opinion for the corresponding fields and LULC class (Fig. 4) where GPS data was already collected (Tab. 2, Column 2). Relative numbers of points per class to be obtained from the ancillary data was determined by visually inspecting the original RapidEye image (Fig. 1); higher numbers of ancillary data points were obtained from the classes with higher spatial coverage. For example, “first crop corn” has the largest spatial coverage, hence higher numbers of data points from ancillary sources were used for ground truthing.

Table 2 - Ground truth data.

Class Name	Original GPS point	Ancillary Data points
First crop corn	11	120
Second crop corn	8	85
Third crop corn	3	10
Well developed cotton	9	100
Moderate developed cotton	4	61
Weak developed cotton	5	50
Wet soil	3	90
Moist soil	5	66
Dry soil	7	66
Water body	2	50
Settlement area	0	65
Pasture and brush land mixed area	3	65
Total	60	828

**Figure 2 - Ground truth from Google Earth.****Figure 3 - Ground truth from Google Earth.**

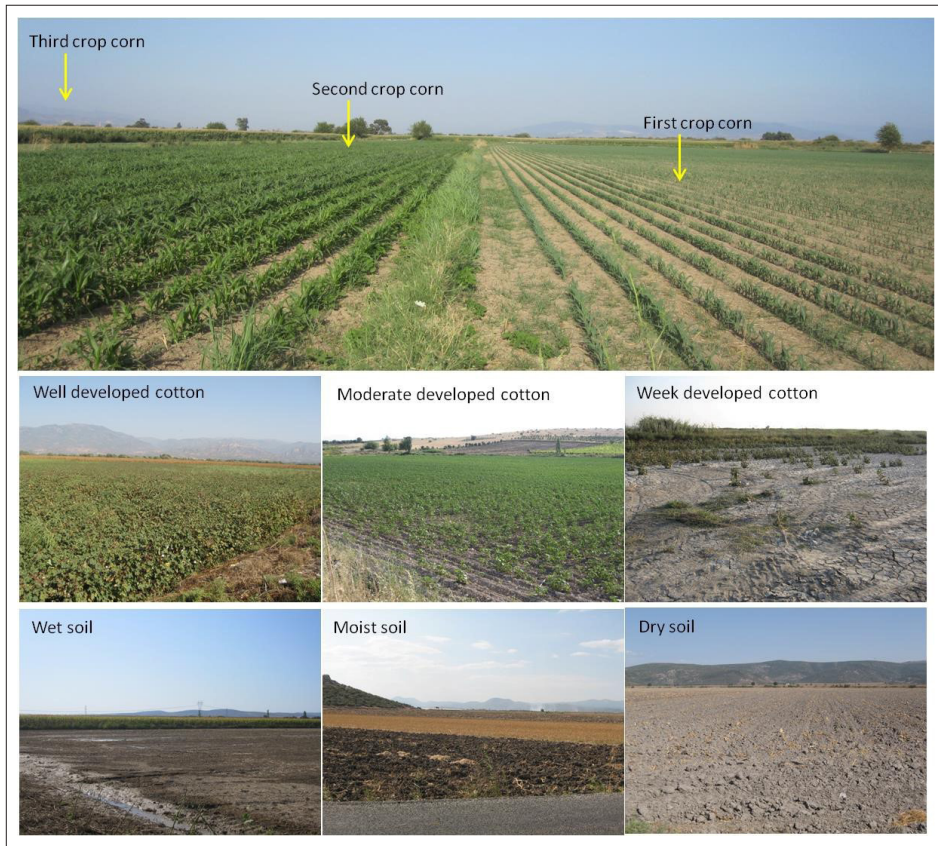


Figure 4 - Crop types in the study area on the acquisition date of RapidEye image (23rd August, 2012).

Classification Strategy and Sensitivity Analysis

The classification was performed with SVMs and MLC classifiers. Classification results of SVMs were compared to traditional methods such as MLC using overall accuracy and kappa index. Sixty-three different models were developed and implemented for sensitivity analysis of SVM architecture based on landuse classification. A total of 63 thematic maps have been produced from various permutations and combinations of configurations of parameters used for sensitivity analysis of SVM architecture. Table 3 summarizes parameters used with SVM architecture.

Pairwise classification strategy (also known as one-against-one voting strategy) has been used here for SVM multiclass classification by ENVI software [ENVI, 2006]. SVM kernels used in this study include linear, polynomial, radial basis function, and sigmoid. The following parameters were identified on SVMs classification, as their optimum selection increased the classification accuracy [Huang et al., 2002; Yang, 2011]: i) error penalty or cost (C) for the all kernels, ii) gamma (γ) for all kernel types except linear, iii) bias term (r) for polynomial and sigmoid kernel, and iv) polynomial degree (d) for polynomial kernel. Figure 5 shows the flowchart of performed study.

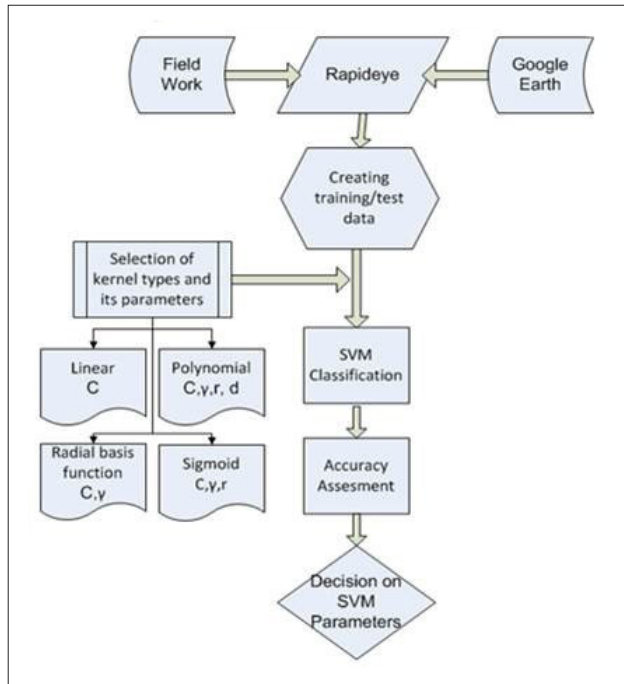


Figure 5 - Flowchart of the study.

Table 3 summarizes SVM models with various kernels and associated parameters used for sensitivity analysis. Error penalty (C) in all the kernels except linear from 0 to 1000 has been arranged increasing in a step of 100. Except the linear kernel, gamma (γ) was fixed to 0.2 which was the inverse of the band number; i.e. RapidEye has five spectral bands, which means gamma is 0.2 as suggested in the ENVI Online Help. The bias from 0 to 7 was used for both polynomial and sigmoid kernels. The polynomial degree was defined from 1 to 6. Since it is difficult to analyse the comparative performance of kernels using common parameters, parameters used in one or more kernels were primarily analyzed to find the optimum values for subsequent analysis. Table 3 summarizes developed models where MLi, MPi, MRi, and MSi stands for model IDs for linear (ML), polynomial (MP), RBF (MR), sigmoid (MS) kernels, respectively.

Table 3 (continued in next pages) - Models for Sensitivity Analysis.

K.Type	Model ID	Poly_degree	Bias	Gamma	Error_Penalty
Linear	ML1	x	x	x	0
	ML2	x	x	x	100
	ML3	x	x	x	200
	ML4	x	x	x	300
	ML5	x	x	x	400
	ML6	x	x	x	500
	ML7	x	x	x	600

Table 3 (continued in next and from preceding page) - Models for Sensitivity Analysis.

K.Type	Model ID	Poly_degree	Bias	Gamma	Error_Penalty
	ML8	x	x	x	700
	ML9	x	x	x	800
	ML10	x	x	x	900
	ML11	x	x	x	1000
Polynomial	MP1	6	5	0.2	0
	MP2	6	5	0.2	100
	MP3	6	5	0.2	200
	MP4	6	5	0.2	300
	MP5	6	5	0.2	400
	MP6	6	5	0.2	500
	MP7	6	5	0.2	600
	MP8	6	5	0.2	700
	MP9	6	5	0.2	800
	MP10	6	5	0.2	900
	MP11	6	5	0.2	1000
	MP12	6	0	0.2	800
	MP13	6	1	0.2	800
	MP14	6	2	0.2	800
	MP15	6	3	0.2	800
	MP16	6	4	0.2	800
	MP17	6	6	0.2	800
	MP18	6	7	0.2	800
	MP19	1	5	0.2	800
	MP20	2	5	0.2	800
Radial Basis Function	MP21	3	5	0.2	800
	MP22	4	5	0.2	800
	MP23	5	5	0.2	800
	MR1	x	x	0.2	0
	MR2	x	x	0.2	100
	MR3	x	x	0.2	200
	MR4	x	x	0.2	300
	MR5	x	x	0.2	400
	MR6	x	x	0.2	500
	MR7	x	x	0.2	600
	MR8	x	x	0.2	700
Sigmoid	MR9	x	x	0.2	800
	MR10	x	x	0.2	900
	MR11	x	x	0.2	1000
	MS1	x	0	0.2	0
	MS2	x	0	0.2	100
	MS3	x	0	0.2	200

Table 3 (continued from preceding pages) - Models for Sensitivity Analysis.

K.Type	Model ID	Poly_degree	Bias	Gamma	Error_Penalty
	MS4	x	0	0.2	300
	MS5	x	0	0.2	400
	MS6	x	0	0.2	500
	MS7	x	0	0.2	600
	MS8	x	0	0.2	700
	MS9	x	0	0.2	800
	MS10	x	0	0.2	900
	MS11	x	0	0.2	1000
	MS12	x	1	0.2	800
	MS13	x	2	0.2	800
	MS14	x	3	0.2	800
	MS15	x	4	0.2	800
	MS16	x	5	0.2	800
	MS17	x	6	0.2	800
	MS18	x	7	0.2	800

Accuracy Assessment

The confusion matrix method, which is used to calculate overall accuracy, and kappa coefficient were used for accuracy assessment. The accuracy of classified images was assessed using 828 ancillary data points that were collected using methods described above. In this study, we used the kappa coefficient as this is considered a useful index to assess the accuracies of classified images against ground truth data [Lorup, 1996; Congalton, 1991].

Results and Discussions

Before discussing the sensitivity of SVMs and its various architectures, the summary of classification accuracy is discussed here based on the best model performance for each category of models (i.e. SVM with Polynomial (MP), SVM with Linear (ML), SVM with Radial Basis Function (MR) and SVM with Sigmoid (MS) as well as MLC). Overall accuracy and overall kappa index for selected SVMs models and MLC are summarized in Figure 6. It is evident from Figure 6 that the SVM model called MP9 (i.e. Polynomial model with 6 degrees of polynomial, bias value of 5, Gamma (γ) of 0.2 and error penalty of 800) produced the classification result with the highest overall accuracy. However, it is difficult to conclude that any type of kernel for SVM can always outperform all other kernel types on classification because the generalization performance of kernels can vary by different remote sensing data sets (multispectral, hyperspectral, SAR etc) depending on training/testing dataset within image classification [Pal, 2012].

Inclusion of the RedEdge band has contributed to the increase on image classification accuracy in our study (Tab. 4). We had 4.6% and 2.4% increases on overall accuracy of SVM and MLC classifications, respectively.

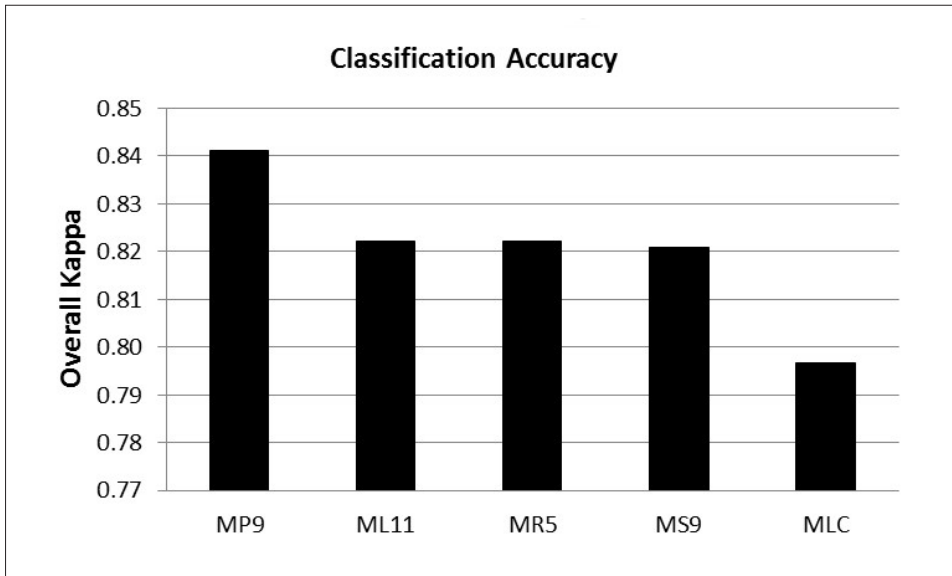


Figure 6 - Classification Accuracy.

Table 4 - Rededge band contribution to accuracy of classification.

Model Name	RedEdge included		RedEdge excluded		Contribution	
	Overall Kappa Index	Overall Accuracy %	Overall Kappa Index	Overall Accuracy %	Overall Kappa Index	Overall Accuracy %
MP9	0.8411	85.63	0.7903	81.04	0.05	4.6
ML11	0.8223	83.94	0.7848	80.55	0.04	3.4
MR5	0.8222	83.94	0.7887	80.92	0.03	3.0
MS9	0.8209	83.82	0.7847	80.55	0.04	3.3
MLC	0.7968	81.64	0.7701	79.23	0.03	2.4

The results indicate that the gamma (γ) term had no impact on classification accuracy, hence, this term will not be analyzed here.

Figure 7 summarizes the classification accuracies based on polynomial degree. The linear kernel (MP19) showed lower accuracy than the nonlinear kernels (MP 20, 21, 22, 23) on classification results. This could be attributed to the nonlinear decision boundaries between the classes since linear kernel (MP19 where $d=1$) is not able to turn nonlinear boundaries to linear ones in the high-dimensional space [Huang et al., 2002]. The classification accuracy usually increased as polynomial degree increased (Fig. 7), with the exception of MP 21.

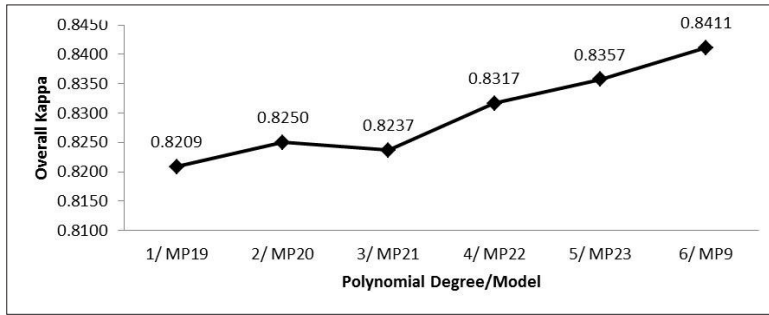


Figure 7 - Polynomial Degree/Model and Overall Kappa.

Table 5 and Table 6 summarize the classification accuracies based on bias. The sixth degree of the kernel with the polynomial model yielded highest classification accuracy. Bias had various impacts on classification accuracy for polynomial kernel (Tab. 5). However when bias has been increased, the classification accuracy has been decreased on sigmoid kernel (Tab. 6). In this study, a bias value of zero with polynomial kernel (MP12) yielded no classification results. MP9 and MS9 produced higher classification accuracy than other level of bias values for polynomial and sigmoid kernels, respectively (Tabs. 5, 6). The classification accuracy usually increased as the bias increased with exception of MP16 with polynomial kernel.

Table 5 - Bias, Model and Overall Kappa for polynomial kernel.

Polynomial	
Bias/Model ID	Overall Kappa
0/MP12	Not performed
1/MP13	0.8249
2/MP14	0.8317
3/MP15	0.8370
4/MP16	0.8344
5/MP9	0.8411
6/MP17	0.8330
7/MP18	0.8304

Table 6 - Bias, Model and Overall Kappa for sigmoid kernel.

Sigmoid	
Bias/Model ID	Overall Kappa
0/MS9	0.8209
2/MS13	0.8115
3/MS14	0.7994
4/MS15	0.7594
5/MS16	0.7327
6/MS17	0.7118
7/MS18	0.6664
2/MS13	0.5483

Table 7 and Table 8 summarize the classification accuracy based on error penalty and kernel type. The models with $i=1$ performed worse than models with $i>1$ for all kernel types. MS9 performed worse than the ML11, MP9, and MR5. MP9 outperformed MS9, MR5 and ML11. Figure 8 shows the classification accuracy (overall kappa) based on error penalty for each kernel type.

Table 7- Error Penalty, Model and Classification accuracy for linear and polynomial kernels.

Linear		Polynomial	
Error Penalty/Model	Kappa	Error Penalty/Model	Kappa
0/ML1	0.7157	0/MP1	0.8101
100/ML2	0.8128	100/MP2	0.8330
200/ML3	0.8209	200/MP3	0.8397
300/ML4	0.8182	300/MP4	0.8331
400/ML5	0.8183	400/MP5	0.8304
500/ML6	0.8170	500/MP6	0.8357
600/ML7	0.8156	600/MP7	0.8304
700/ML8	0.8169	700/MP8	0.8344
800/ML9	0.8209	800/MP9	0.8411
900/ML10	0.8183	900/MP10	0.8357
1000/ML11	0.8223	1000/MP11	0.8330

Table 8 - Error Penalty, Model and Classification accuracy for radial basis function and sigmoid kernels.

Radial Basis Function		Sigmoid	
Error Penalty/Model	Kappa	Error Penalty/Model	Kappa
0/MR1	0.6907	0/MS1	0.6906
100/MR2	0.8128	100/MS2	0.8034
200/MR3	0.8155	200/MS3	0.8142
300/MR4	0.8182	300/MS4	0.8128
400/MR5	0.8222	400/MS5	0.8128
500/MR6	0.8222	500/MS6	0.8128
600/MR7	0.8209	600/MS7	0.8115
700/MR8	0.8209	700/MS8	0.8155
800/MR9	0.8196	800/MS9	0.8209
900/MR10	0.8209	900/MS10	0.8209
1000/MR11	0.8209	1000/MS11	0.8209

Figure 8 shows the sensitivity of classification accuracy to error penalty.

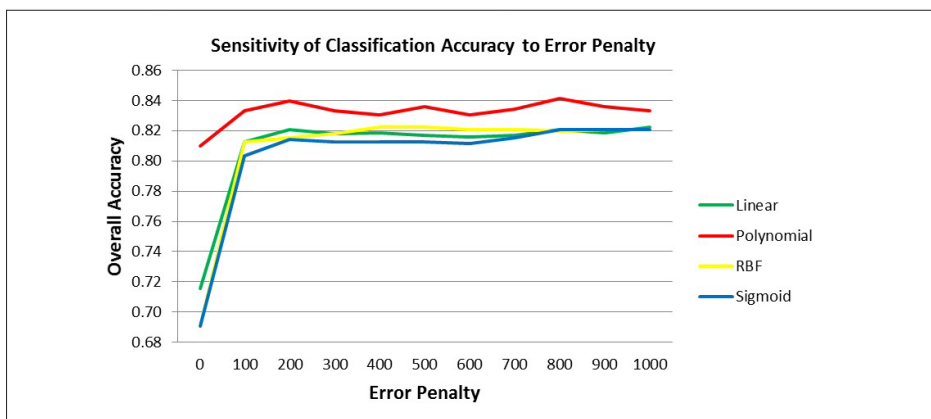


Figure 8 - Sensitivity of classification accuracy with different Error Penalty per Kernel type.

Figure 9 shows the landuse/landcover thematic maps for the MS9, MR5, ML11, MP9 and MLC.

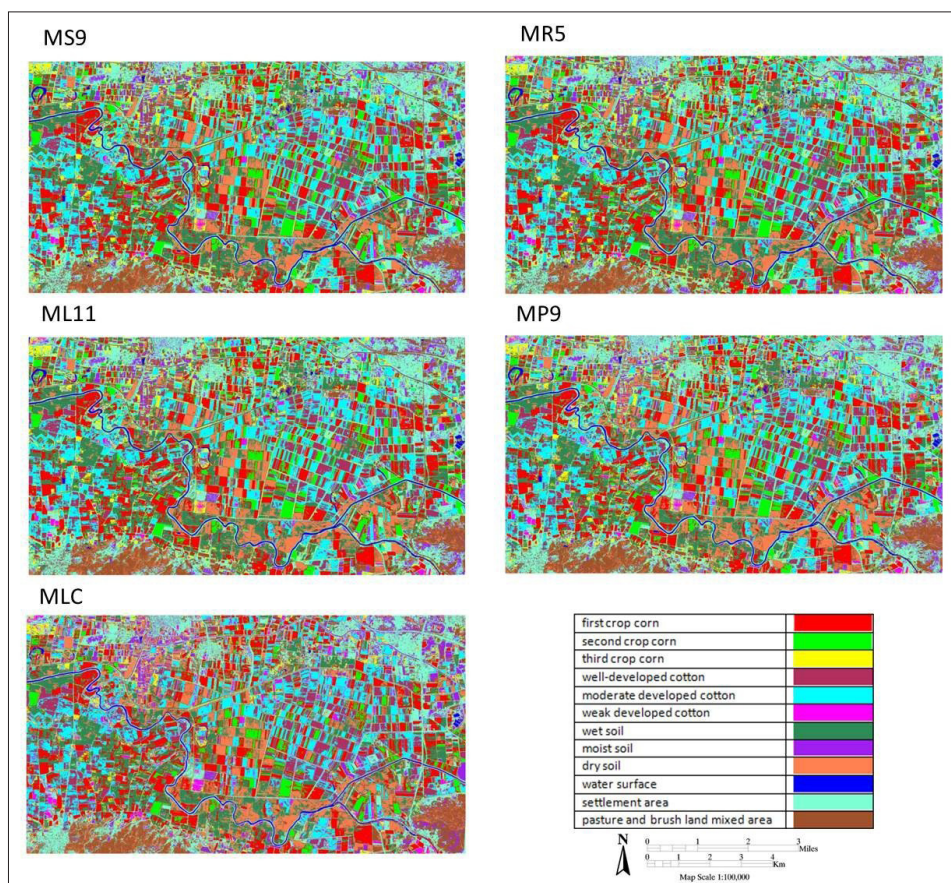


Figure 9 - Classified Maps from RapidEye Image.

Table 9 summarizes the percentage of area coverage for class category on MLC, ML11, MP9, MR5 and MS9. Wet soil and weak developed cotton showed the most critical changes of percentage area coverage, this could be attributed to the signature overlaps (Tab. 9).

Table 9 - Percentage of area coverage.

Class	MLC %	ML11 %	MP9 %	MR5 %	MS9 %	Change in all methods %
first crop corn	15.40	14.60	14.30	14.30	14.30	1.10
second crop corn	2.90	4.00	3.90	4.20	4.20	1.30
third crop corn	4.80	6.20	5.90	6.70	6.70	1.90
well-developed cotton	7.00	6.20	6.20	6.30	6.30	0.80
moderate developed cotton	14.00	16.10	15.70	16.00	16.00	2.10
weak developed cotton	4.90	2.00	2.80	2.00	2.00	2.90
wet soil	14.90	15.80	14.20	16.50	16.60	2.40
moist soil	4.20	3.50	3.10	3.30	3.20	1.10
dry soil	9.80	8.20	9.50	7.60	7.60	2.20
pasture and brush land mixed area	6.30	7.20	6.50	7.20	7.30	1.00
water surface	1.00	1.30	1.40	1.30	1.30	0.40
settlement area	14.90	15.10	16.50	14.70	14.60	1.90

Additionally, the Kappa statistic tool from Map Comparison Kit (MCK), a freeware program developed by Research Institute for Knowledge Systems BV (RIKS), has been applied to assess the differences between raster maps; namely equal and unequal areas between resultant thematic maps (MLC, ML11, MP9, MR5, MS9). MCK can be downloaded for free at <http://www.mck.riks.nl> and details about software are provided in Visser and Nijs [2006]. In this statistical tool, Kappa refers to the agreement ratio between classified images. Equal-unequal maps in Figure 10 shows the differences between two maps with Kappa values. Each map was compared with the other ones.

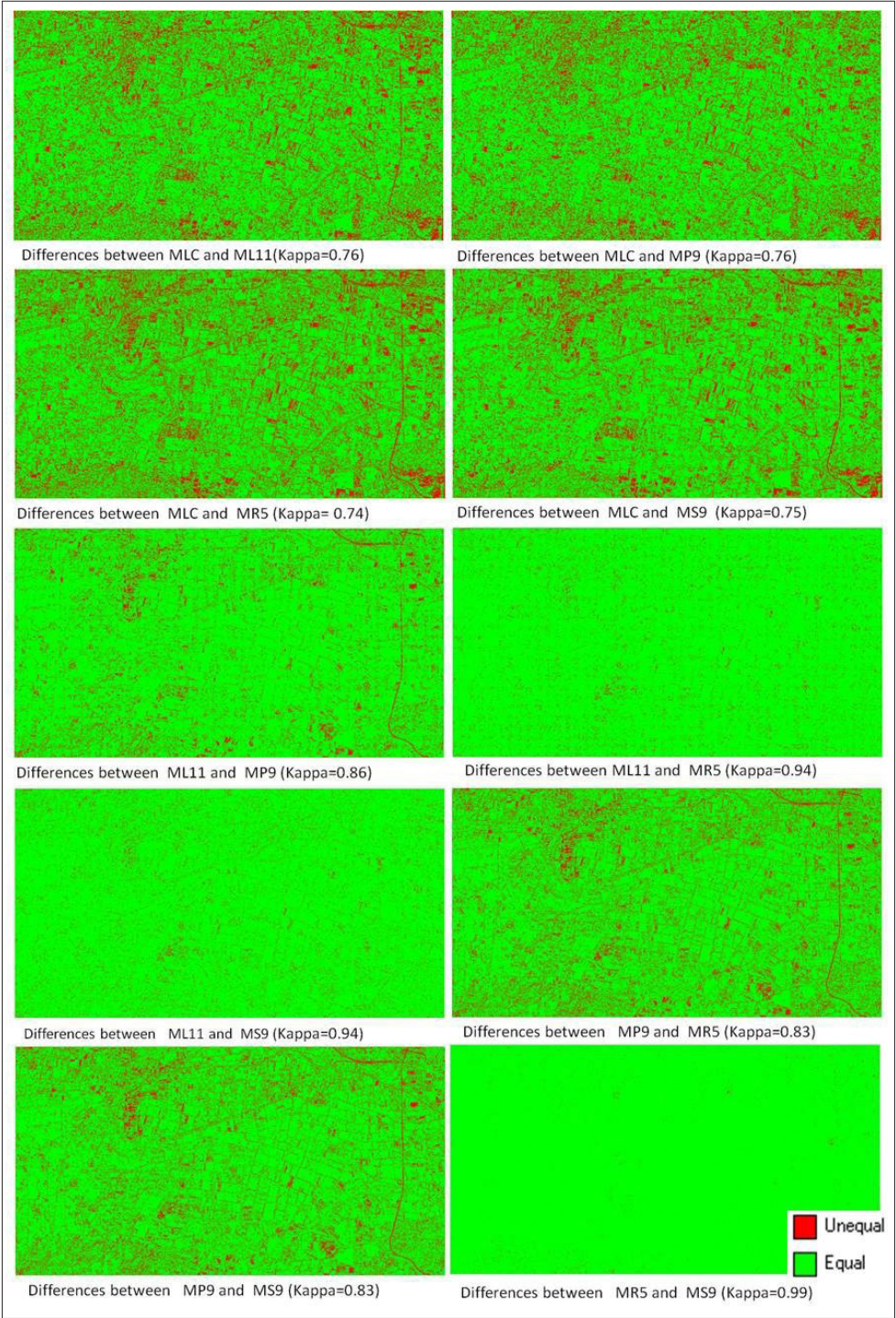


Figure 10 - Differences between maps and kappa values.

As seen in Figure 10, kappa values between SVMs methods are higher than values between SVMs and MLC, especially MR5 and MS9 show high similarity. MS9 is characterized by an error penalty of 800, Gamma of 0.2 and bias of 0, whereas MR5 is characterized by an error penalty of 400 and Gamma of 0.2. Overall accuracies of ML11, MR5, and MS9 are about 83%, whereas MP9 showed 85% of overall accuracy. MLC showed the least overall accuracy of 81% compared to SVMs models used in this study.

Conclusions

In this paper, the sensitivity of SVM architecture has been investigated by using high-resolution RapidEye image for the area covering twelve LULC classes of Aydin Province, Turkey. For this study, 63 different models were developed to conduct sensitivity analysis. As proven in previous studies, RapidEye data has been successfully used for precision agriculture using image classification and the results are satisfactory. Various trials have been carried out to construct the kernel configurations due to the absence of a priori information regarding optimum parameters.

When compared, the classification accuracies of selected SVM models (ML11, MP9, MR5 and MS9), MP9 and MS9 had relatively higher (85.6%) and relatively lower (83.8%) classification accuracy, respectively. ML11 and MR5 showed equal performance in terms of overall accuracy (83.9%), whereas MLC showed overall accuracy of 81.6%. It can be concluded that error penalty and kernel type have critical importance on sensitivity of SVM architecture. Optimum parameters vary from data to data and method to method used in classification. Therefore it is recommended that the optimum parameters for SVM models should be analyzed in detail before selecting the final models for the best classification results.

We can conclude that RapidEye imagery gives satisfactory results for classification on agricultural applications and SVMs can accomplish high classification accuracy with a small size of training datasets. SVM models in all selected cases (best per class for each of the four models: linear, polynomial, radial basis function, and sigmoid) outperformed the traditional MLC method.

Acknowledgements

Authors gratefully acknowledge to Prof. Dr. Yusuf Kurucu and Dr. M. Tolga Esetlili from the Department of Soil Science and Plant Nutrition in Ege University, for providing free access to satellite imagery and ground truth data for the study area as well as helping out at the interpretation of the crop types within this study. We would also like to thank anonymous reviewers for their insightful comments and suggestions.

References

- Abdikan S., Bilgin G., Sanli F.B., Uslu E., Ustuner M. (2015) - *Enhancing land use classification with fusing dual-polarized TerraSAR-X and multispectral RapidEye data.* Journal of Applied Remote Sensing, 9: 096054-096054. doi: <http://dx.doi.org/10.1117/1.JRS.9.096054>.
- Adam E., Mutanga O., Odindi J., Abdel-Rahman E.M. (2014) - *Land-use/cover classification in a heterogeneous coastal landscape using RapidEye imagery: evaluating the*

- performance of random forest and support vector machines classifiers*. International Journal of Remote Sensing, 35: 3440-3458. doi: <http://dx.doi.org/10.1080/01431161.2014.903435>.
- Adelabu S., Mutanga O., Adam E. (2014) - *Evaluating the impact of red-edge band from Rapideye image for classifying insect defoliation levels*. ISPRS Journal of Photogrammetry and Remote Sensing, 95: 34-41. doi: <http://dx.doi.org/10.1016/j.isprsjprs.2014.05.013>.
- Agricultural Research and Extension Council of Alberta (2010) - *Precision Farming and Variable Rate Technology*. Available online at: http://areca.ab.ca/userfiles/files/VRT_Resource_Manual_Mar_2010.pdf. (last accessed 30.04.2014).
- BlackBridge (2013) - *RapidEye Satellite Imagery Product Specifications, Version 6*. Available online at: http://www.blackbridge.com/rapideye/upload/RE_Product_Specifications_ENG.pdf.
- Cortes C., Vapnik V. (1995) - *Support-Vector Networks*. Machine Learning, 20: 273-297. doi: <http://dx.doi.org/10.1007/BF00994018>.
- Congalton R.G. (1991) - *A review of assessing the accuracy of classifications of remotely sensed data*. Remote Sensing of Environment, 37: 35-46. doi: [http://dx.doi.org/10.1016/0034-4257\(91\)90048-B](http://dx.doi.org/10.1016/0034-4257(91)90048-B).
- Conrad C., Dech S., Dubovyk O., Fritsch S., Klein D., Löw F., Schorcht G., Zeidler J. (2014) - *Derivation of temporal windows for accurate crop discrimination in heterogeneous croplands of Uzbekistan using multitemporal RapidEye images*. Computers and Electronics in Agriculture, 103: 63-74. di: <http://dx.doi.org/10.1016/j.compag.2014.02.003>.
- Dixon B., Candade N. (2007) - *Multispectral landuse classification using neural networks and support vector machines: one or the other, or both?* International Journal of Remote Sensing, 29: 1185-1206. doi: <http://dx.doi.org/10.1080/01431160701294661>.
- ENVI (2006) - *Online Help, Applying Support Vector Machine Classification*. Available online at: http://gridkr.com/d/ENVI_4_3/online_help/ApplyingSVMClassification.html (last accessed: 30.04.2014)
- European Environment Agency (2010) - *The European environment - state and outlook 2010*. Available online at: http://www.eea.europa.eu/soer/countries/tr/soertopic_view?topic=land (last accessed: 30.04.2014).
- Forkuor G., Conrad C., Thiel M., Ullmann T., Zoungrana E. (2014) - *Integration of Optical and Synthetic Aperture Radar Imager for Improving Crop Mapping in Northwestern Benin, West Africa*. Remote Sensing, 6: 6472-6499. doi: <http://dx.doi.org/10.3390/rs6076472>.
- Hall F.G., Townshend J.R., Engman E.T. (1995) - *Status of remote sensing algorithms for estimation of land surface state parameters*. Remote Sensing of Environment, 51: 138-156. doi: [http://dx.doi.org/10.1016/0034-4257\(94\)00071-T](http://dx.doi.org/10.1016/0034-4257(94)00071-T).
- Huang C., Davis L.S., Townshend J.R.G. (2002) - *An assessment of support vector machines for land cover classification*. International Journal of Remote Sensing, 23: 725-749. doi: <http://dx.doi.org/10.1080/01431160110040323>.
- Weeber J. (2010) - *RapidEye Satellite Imaging System, Defense/Intelligence Capabilities*. Available online at: http://usgif.org/system/uploads/1009/original/John_Weeber.pdf (last accessed: 27.08.2014).

- Kavzoglu T., Colkesen I. (2009) - *A kernel functions analysis for support vector machines for land cover classification*. International Journal of Applied Earth Observation and Geoinformation, 11: 352-359. doi: <http://dx.doi.org/10.1016/j.jag.2009.06.002>.
- Lorup E.J. (1996) - *Crosstabulation*. Available online at: <http://uhaweb.hartford.edu/gatetutor/idrisi/mptools2.html> (last accessed: 30.04.2014).
- Löw F., Michel U., Dech S., Conrad C. (2013) - *Impact of feature selection on the accuracy and spatial uncertainty of per-field crop classification using Support Vector Machines*. ISPRS Journal of Photogrammetry and Remote Sensing, 85: 102-119. doi: <http://dx.doi.org/10.1016/j.isprsjprs.2013.08.007>.
- Löw F., Knöfel P., Conrad C. (2015) - *Analysis of uncertainty in multi-temporal object-based classification*. ISPRS Journal of Photogrammetry and Remote Sensing, 105: 91-106. doi: <http://dx.doi.org/10.1016/j.isprsjprs.2015.03.004>.
- Mather P.M. (2001) - *Computer processing of Remotely-Sensed images: An Introduction*. New York: John Wiley & Sons.
- Mathur A., Foody G.M. (2008) - *Crop classification by support vector machine with intelligently selected training data for an operational application*. International Journal of Remote Sensing, 29: 2227-2240. doi: <http://dx.doi.org/10.1080/01431160701395203>.
- McNairn H., Ellis J., Van Der Sanden J.J., Hirose T., Brown R.J. (2002) - *Providing crop information using RADARSAT-1 and satellite optical imagery*. International Journal of Remote Sensing, 23: 851-870. doi: <http://dx.doi.org/10.1080/01431160110070753>.
- Mountrakis G., Im J., Ogole C. (2011) - *Support vector machines in remote sensing: A review*. ISPRS Journal of Photogrammetry and Remote Sensing, 66: 247-259. doi: <http://dx.doi.org/10.1016/j.isprsjprs.2010.11.001>.
- Otakei J.R., Blaschke T. (2010) - *Land cover change assessment using decision trees, support vector machines and maximum likelihood classification algorithms*. International Journal of Applied Earth Observation and Geoinformation, 12 (1): S27-S31. doi: <http://dx.doi.org/10.1016/j.jag.2009.11.002>.
- Pal M., Mather P.M. (2004) - *Assessment of the effectiveness of support vector machines for hyperspectral data*. Future Generation Computer Systems, 20: 1215-1225. doi: <http://dx.doi.org/10.1016/j.future.2003.11.011>.
- Pal M., Mather P.M. (2005) - *Support vector machines for classification in remote sensing*. International Journal of Remote Sensing, 26: 1007-1011. doi: <http://dx.doi.org/10.1080/01431160512331314083>.
- Pal M. (2012) - *Advanced algorithms for land use and cover classification*. Advances in Mapping from Remote Sensor Imagery, CRC Press, pp. 69-90. doi: <http://dx.doi.org/10.1201/b13770-4>.
- Petropoulos G.P., Kalaitzidis C., Prasad Vadrevu K. (2012) - *Support vector machines and object-based classification for obtaining land-use/cover cartography from Hyperion hyperspectral imagery*. Computers & Geosciences, 41: 99-107. doi: <http://dx.doi.org/10.1016/j.cageo.2011.08.019>.
- Rogan J., Chen D. (2004) - *Remote sensing technology for mapping and monitoring land-cover and land-use change*. Progress in Planning, 61: 301-325. doi: [http://dx.doi.org/10.1016/S0305-9006\(03\)00066-7](http://dx.doi.org/10.1016/S0305-9006(03)00066-7).
- Roscher R., Förstner W., Waske B. (2012) - *I2VM: Incremental import vector machines*. Image and Vision Computing, 30: 263-278. doi: <http://dx.doi.org/10.1016/>

- j.imavis.2012.04.004.
- Sandau R. (2010) - *Status and trends of small satellite missions for Earth observation*. Acta Astronautica, 66: 1-12. doi: <http://dx.doi.org/10.1016/j.actaastro.2009.06.008>.
- Schuster C., Förster M., Kleinschmit B. (2012) - *Testing the red edge channel for improving land-use classifications based on high-resolution multi-spectral satellite data*. International Journal of Remote Sensing, 33: 5583-5599. doi: <http://dx.doi.org/10.1080/01431161.2012.666812>.
- Schuster C., Schmidt T., Conrad C., Kleinschmit B., Förster M. (2015) - *Grassland habitat mapping by intra-annual time series analysis - Comparison of RapidEye and TerraSAR-X satellite data*. International Journal of Applied Earth Observation and Geoinformation, 34: 25-34. doi: <http://dx.doi.org/10.1016/j.jag.2014.06.004>.
- Soria-Ruiz J., Fernandez-Ordenez Y., McNairn H. (2009) - *Corn Monitoring and Crop Yield Using Optical and Microwave Remote Sensing*. In Ho P-G. P. (Ed.), Geoscience and Remote Sensing, InTech, Open Access Publisher, Chapter 19. doi: <http://dx.doi.org/10.5772/8311>.
- Tigges J., Lakes T., Hostert P. (2013) - *Urban vegetation classification: Benefits of multitemporal RapidEye satellite data*. Remote Sensing of Environment, 136: 66-75. doi: <http://dx.doi.org/10.1016/j.rse.2013.05.001>.
- Townshend J.R.G. (1992) - *Land cover*. International Journal of Remote Sensing, 13: 1319-1328. doi: <http://dx.doi.org/10.1080/01431169208904193>.
- Tyc G., Tulip J., Schulten D., Krischke M., Oxfort M. (2005) - *The RapidEye mission design*. Acta Astronautica, 56: 213-219. doi: <http://dx.doi.org/10.1016/j.actaastro.2004.09.029>.
- Unal E., Mermer A., Urla O., Ceylan N., Yildiz H., Aydogdu M. (2006) - *Pilot study on wheat area estimates in Turkey*. ISPRS WG VIII/10 Workshop 2006: 135-138.
- Vapnik V.N. (1995) - *The nature of statistical learning theory*. Springer, New York. doi: <http://dx.doi.org/10.1007/978-1-4757-2440-0>.
- Visser H., de Nijs T. (2006) - *The Map Comparison Kit*. Environmental Modelling & Software, 21: 346-358. doi: <http://dx.doi.org/10.1016/j.envsoft.2004.11.013>.
- Watanachaturaporn P., Arora M.K., Varshney P.K. (2008) - *Multisource classification using support vector machines: an empirical comparison with decision tree and neural network classifiers*. Photogrammetric Engineering & Remote Sensing, 74 (2): 239-246. doi: <http://dx.doi.org/10.14358/PERS.74.2.239>.
- Yang X. (2011) - *Parameterizing Support Vector Machines for Land Cover Classification*. Photogrammetric Engineering & Remote Sensing, 77: 27-37. doi: <http://dx.doi.org/10.14358/PERS.77.1.27>.

© 2015 by the authors; licensee Italian Society of Remote Sensing (AIT). This article is an open access article distributed under the terms and conditions of the Creative Commons Attribution license (<http://creativecommons.org/licenses/by/4.0/>).